International Journal of Mechanics and Energy (IJME)
Vol. 1, Issue 4, 2013, ISSN: 2286-5845

Numerical modeling of microfluidic flow through a channel with sensitive membrane

Marwa Selmi, F. Echouchene*, H.Mejri, and H. Belmabrouk

Electronic and Microelectronic Laboratory/department of Physics, Faculty of Science of Monastir, Monastir University, Monastir, Tunisia

Received June 5, 2012 / Accepted September 9, 2012 / Published January 8, 2012.

Abstract: The binding reaction is a significant characteristic which is adopted in the design of biosensors. This aim of the present work is to investigate the binding reaction kinetics through a microchannel. The diffusion boundary layer on the reaction surface of a biosensor operating in fluid environment, presents restraining effects. Therefore, it is useful to optimize several critical parameters, which affect the binding reaction such as, the length of the reaction surface, the inlet flow velocity, and the initial biological analyte concentration (e.g. molecule, protein, toxin, peptide, vitamin, sugar, metal ion…) in order to reduce the thickness of the diffusion boundary layer. The study is performed using 2D finite element method. Then, the space-time evolution of analyte concentration (such as C-reactive protein or IgG) is simulated. The results prove that the reaction kinetic is strongly affected and hence the diffusion boundary layer is assigned by the physical and geometrical parameters of the microfluidic biosensor.

Key words: Binding reaction, microfluidic systems, biosensors, finite element method, biological analytes, simulation.

1. Introduction

Microfluidics have became over the last decade a veritable science in full swing [1-13]. Their development has been conditioned by the technological possibility of adapting microfabrication techniques originally designed for electronic fluidic applications. Microfluidic devices possess many of the features that make bioassays advantageous, short analysis time, and the ability to operate with small samples and high sensitivity [4, 5]. Biosensors are sensing devices that incorporate a biological sensing element and a transducer producing an electrochemical, optical, or other signal in proportion to quantitative information about the analytes in the given medium [14-17]. The function of a biosensor depends on the biochemical specificity of the biologically active material. The binding reaction is a significant characteristic that is applied to design biosensors. The diffusion boundary layer on the reaction surface of a biosensor operating in fluid environmen presents restraining effects.

The paper reports on a numerical simulation of microfluidic flow through a channel with a sensitive membrane. For a designed microfluidic channel, the surface concentration distribution is simulated using finite element method. The effects of initial velocity, initial analyte concentration and the surface reaction length are analyzed with the aim to improve the sensitivity of the biosensor to model.

2. Physical model

The system to model consists in a two-dimensional biosensor in a microchannel (see Fig. 1). The height and the length of the microchannel are denoted by h and L. The system mixes a small concentration of a biological analyte with the fluid in a microchannel where a surface reaction is located. The fluid flows from the left to the right.

To analyze the binding reaction on the biosensor surface, the fluid flow, electrochemistry and mass

*** Corresponding author:** Fraj Echouchene
E-mail: frchouchene@yahoo.fr.

transport, and reaction surface models are coupled and solved numerically.

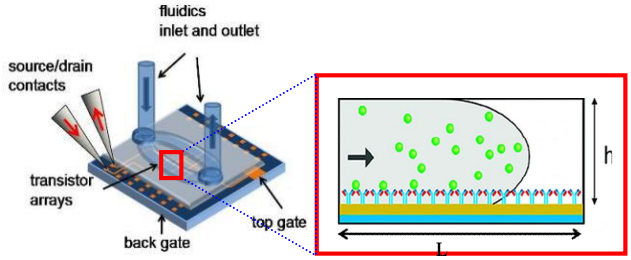

Fig. 1 Schematic depiction of a microfluidic device: single-channel and detection surface.

2.1 Fluid flow model

The flow is assumed to be study, isothermal, incompressible and the fluid is Newtonian.

a-Continuity equation

The mass conservation equation of the flow in *x*-*y* cartesian coordinates reads as:

$$\frac{\partial u}{\partial x}+\frac{\partial v}{\partial y}=0 \tag{1}$$

where u and v are the x and the y velocity components respectively.

b-Momentum conservation equation

The Navier Stocks equations can be written under the form :

$$\begin{cases}\rho\left(\dfrac{\partial u}{\partial t}+u\dfrac{\partial u}{\partial x}+v\dfrac{\partial u}{\partial y}\right)=-\dfrac{\partial p}{\partial x}+\eta\nabla^2 u\\ \rho\left(\dfrac{\partial v}{\partial t}+u\dfrac{\partial v}{\partial x}+v\dfrac{\partial v}{\partial y}\right)=-\dfrac{\partial p}{\partial y}+\eta\nabla^2 v\end{cases} \tag{2}$$

where η is the dynamic viscosity of fluid, ρ is the fluid density and p is the static pressure. The viscosity and the density of fluid are assumed to be constant.

2.2 Electrochemistry and mass transport model

Transport of analytes towards the reaction surface can be described using the Fick second law with convective terms:

$$\frac{\partial[A]}{\partial t}+div(-D\overrightarrow{grad}[A])+div\left([A]\vec{u}\right)=0 \tag{3}$$

where $[A]$ represents the analyte concentration and D is the diffusion coefficient of analytes in the bulk.

2.3 The reaction surface

The reaction between immobilized ligands and analytes is assumed to follow the first order Langmuir adsorption model [18, 19]:

$$\frac{\partial[AB]}{\partial t}+div(-D_s\overrightarrow{grad}[AB])=k_a[A]_s\{[B_0]-[AB]\}-k_d[AB] \tag{4}$$

where $[A]_s$ is the analyte concentration at the reaction surface by mass-transport, $[B_0]$ is the initial ligand concentration at the surface, and $[AB]$ is the anlytee-ligand complex concentration.

3. Boundary and initial conditions

The fluid used in our simulation is the water whose dynamic viscosity η is equal to 10^{-3} Pa.s and the density is 10^3 kg/m^3. Since the flow in the microchannel is in a low Reynolds number condition, it is assumed to be a laminar flow. The average velocity of the parabolic is assumed to be variable at the inlet of the microchannel. At the outlet section, static pressure is adopted as boundary condition, and nonslip elsewhere. The fluid is assumed to be at rest initially.

For the mass-transport equation, the boundaries conditions are:

i. At the inlet, the analyte concentration $[A_0]$ is applied;
ii. At the reaction surface, the diffusion flux is balanced against the reaction rate;
iii. The convective flux is adopted at the outlet;
iv. On the walls, the insulation boundary condition is applied.

Initially, the analyte concentration is equal to zero. Diffusion coefficient of analyte is taken as 10^{-11} m^2/s. The inlet concentration is chosen as $[A]$=1µmol/m^3. The initial surface concentration is $[B_0]$.

4. Numerical method

In simulating the flow within the microfluidic channel, the governing equations and the initial, and boundary conditions were solved using the finite element method using the software Comsol Multiphysics [20]. The

discretized algebraic equations were then solved using the UMFPACK (unsymmetric multifrontal sparse LU factorization package) direct solver. A quadratic discretization scheme is used for all the mass transport. In the solution procedure, the Navier-Stokes equations (i.e., Eqs. (1) and (2)) were firstly solved to calculate the evolution of the flow field over time. Based on the previous results of Navier-Stokes equations, the convection–diffusion and kinetic equations (i.e., Eqs. (3) and (4)) were then solved concurrently to obtain the concentration field of analyte within the microchannel and the analyte-ligand complex concentration on the reaction surface.

5. Results and discussions

Figure 2 shows the profile of the complex analyte-ligand concentration versus time during the association process. Usually, biosensors should operate in a short time. Numerical simulation is carried out after 5 seconds. Throughout this period, the concentration profile of the complexe is similar to the diode response. We can deduce from this curve a critical parameter: the threshold time. The latter is the time from which analytes arranges with ligands to produce a complex.

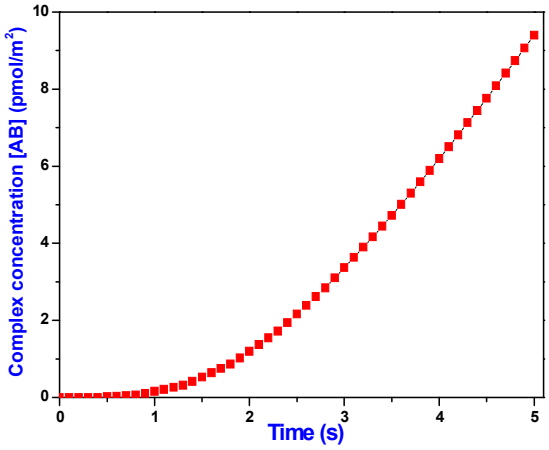

Fig. 2 Binding of molecules on the reaction surface in the microchannel.

Figure 3 shows the flow profile and the concentration distribution just 1, 2.5, 5, and 10 s after introducing the analyte.

In this case, the flow profile is laminar and has a parabolic profile. From time t = 2.5s a portion of the analyte diffuses towards the reaction surface. A portion of the diffused analyte is associated with the ligands forming the complex. At the sensitive membrane, the analyte concentration is minimal since it is attached with the ligands.

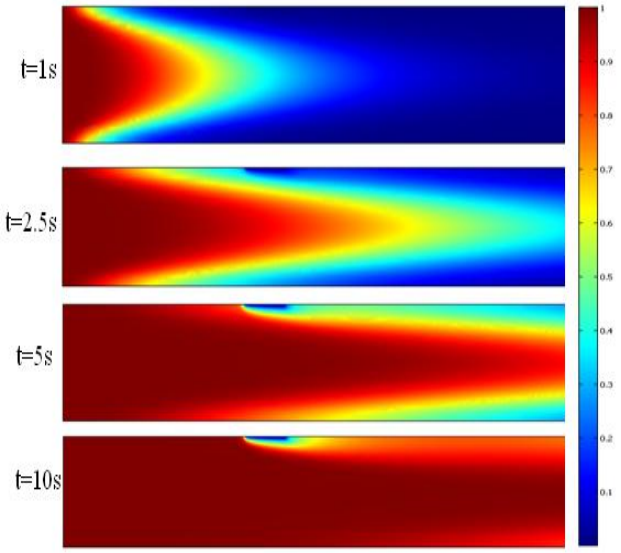

Fig. 3 Diffusion of the analytes in the microchannel at different times.

Several critical parameters, can affect the binding reaction such as, the reaction surface length, the inlet flow velocity, and the initial analyte concentration. In the following work, we will investigate the influence of these parameters at the binding reaction

5.1 Inlet velocity flow effect

The incoming flow profile is characteristic for fully developed laminar flow, that is, parabolic with zero velocity at the channel walls. The average velocity of the parabolic pofile is noted u_{max}. Figure 4 shows the time evolution of analyte-ligand concentration for several inlet flow velocities (u_{max}=10^{-4}, 10^{-3}, and 10^{-2} m/s). The diffusion velocity of many biomolecules is relatively slow compared to the reaction velocity, as measured by the Damkoehler number (D_a number). The latter is the ratio of the reaction velocity (i.e., product of the association rate constant and the initial concentration of

the ligand) to diffusion velocity. When the D_a number is greater than unity, the whole reaction is restrained by diffusion. In figure 4, the concentration of the complexe is strongly influenced by the inlet velocity u_{max}. When the inlet velocity increases, the diffusion boundary layer is reduced and therefore, the reaction surface increases. In conclusion, the inlet velocity plays a crucial role in reducing the diffusion boundary layer.

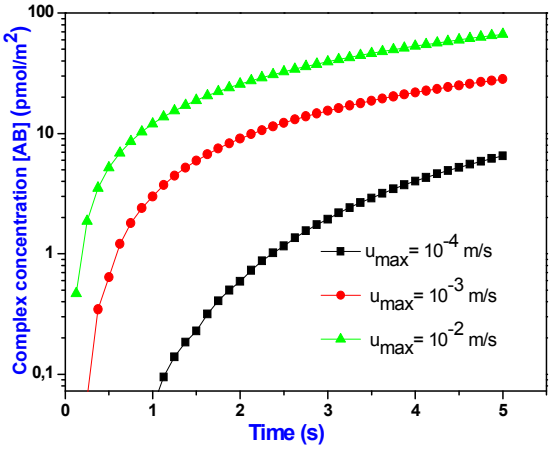

Fig. 4 Influence of the inlet flow velocity on the binding of molecules on the reaction surface vs. time.

5.2 Effect of analyte initial concentration

Figure 5 reveals the profiles of the concentration of analyte-ligand complex along the surface vs time for different analyte bulk concentrations.

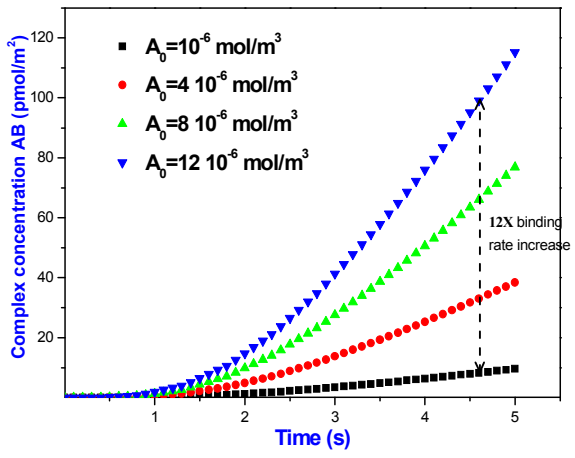

Fig. 5 Influence of initial analyte-bulk on the binding of molecules on the reaction surface vs. time.

The analyte bulk concentrations used in this simulation are $[A_0] = [1, 4, 8, 12]\mu mol/m^3$. Figure 5 shows that the binding reaction is faster when the analyte bulk concentration $[A_0]$ is significant.

For the initial analyte concentration range studied, the complex concentration varies linearly (Fig. 6).

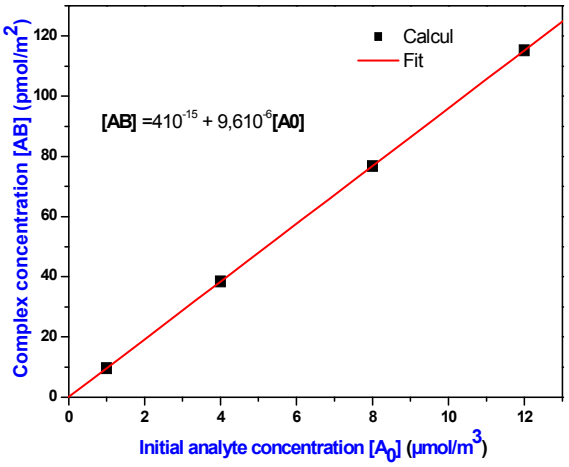

Fig. 6 Analyte-ligand complex concentration [AB] at t =5s versus the initial analyte concentration $[A_0]$.

5.3 Effect of surface reaction length

In this subsection, the surface reaction length is allowed to vary. Figure 7 illustrates the temporel evolution of the complex concentration for several surface reaction lengths.

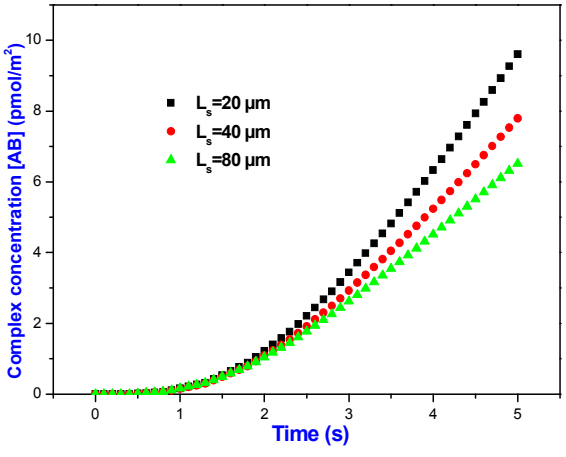

Fig. 7 Effect of reaction surface lengths on the binding of molecules on the reaction surface vs. time.

Three values of surface reaction lengths are used in this simulation: L_s=20, 40, 80µm. The inlet analyte concentration and the inlet velocity are assumed constant. Figure 7 proves that the length of the reaction surface plays an important role in the formation of the diffusion boundary layer. resulting in a slower binding rate and a longer time to reach saturation. When increasing the reaction surface at the same time keeping the concentration of the ligands fixed, this induces a reduction of the particle density. The decrease in particle density leads a slowdown in the rate of ligand-analyte reaction.

5. Conclusion

This work presents 2D numerical simulation of a microfluidic in microchannel containing a sensitive membrane by using the finite elements method. Several crucial factors have been evoked: the inlet flow velocity, the initial analyte concentration, and the length of reaction surface. Results prove that the binding reaction strongly depend on geometrical and physical parameters of the micro-fluidic system used.

References

[1] G. M. Whitesides, The Origins and the Future of Microfluidics, Nature 442 (2006) 368-373.

[2] P. Tabeling, Introduction to microfluidics, Oxford University Press, USA (2005).

[3] T. M. Squires and S. R. Quake, Microfluidics: Fluid Physics at the Nanoliter Scale, Rev. Mod. Phys, 77 (2005) 977-1026.

[4] C.C. Lin, J.H. Wang, H.W. Wu, G.B. Lee, J. JALA. Assoc. Lab. Autom, 15 (3) (2010) 253-274.

[5] A. Ng.H.C, U. Uddayasankar, A.R. Wheeler, Immunoassays in Microfluidic Systems Anal, Bioanal. Chem, 397 (2010) 991-1007.

[6] B. V. Chikkaveeraiah, V. Mania, V. Patel, J. Silvio Gutkind, J. F. Rusling, Microfluidic Electrochemical Immunoarray for Ultrasensitive Detection of two Cancer Biomarker Proteins in Serum, Biosensors and Bioelectronics, 26 (2011) 4477-4483.

[7] P. Chandra, S. Abbas Zaidi, H-B. Noh, Y-B. Shim, Separation and Simultaneous Detection of Anticancer Drugs in a Microfluidic Device with an Amperometric Biosensor, Biosensors and Bioelectronics, 28 (2011) 326–332.

[8] Y-C. Chuang, K-C. Lan, K-M. Hsieh, L-S. Jang, M-K. Chen, Detection of Glycated Hemoglobin (HbA1c) based on Impedance Measurement with Parallel Electrodes Integrated into a Microfluidic device. Sensors and Actuators B, 171-172 (2012) 1222–1230.

[9] C. Dalmay, J. Villemejane, V. Joubert, O. Français, L. M. Mir, B. Le Pioufle, Design and Realization of a Microfluidic device devoted to the Application of Ultra-short Pulses of Electrical Field to Living Cells, Sensors and Actuators B 160 (2011) 1573-1580.

[10] Y. Date, S. Terakado, K. Sasaki, A. Aota, N. Matsumotoa, H. Shiku, K. Ino, Y. Watanabea, T. Matsue, N. Ohmura, Microfluidic Heavy Metal Immunoassay based on Absorbance Measurement, Biosensors and Bioelectronics, 33 (2012) 106-112.

[11] Z. Fekete, P. Nagy, G. Huszka, F. Tolner, A. Pongrácz, P. Fürjes, Performance Characterization of Micromachined Particle Separation System based on Zweifach–Fung effect, Sensors and Actuators B 162 (2012) 89-94.

[12] Y. Murakami, T. Endo, S. Yamamura, N. Nagatani, Y. Takamura, E. Tamiya, On-chip Micro-Xow Polystyrene Bead-based Immunoassay for quantitative Detection of Tacrolimus (FK506), Analytical Biochemistry, 334 (2004) 111–116.

[13] L. Gervais, E. Delamarche, Toward one-step point-of-care Immunodiagnostics using Capillary-driven Microfluidics and PDMS Substrates, Lab Chip: Miniaturisation Chem. Biol, 9 (23) (2009) 3330-3337.

[14] A. P.F.Turner, I. Karube,. G.S. Wilson. Biosensors: Fundamentals and Applications (Eds.), Oxford University Press, Ox-ford, UK (1987).

[15] L.J. Blum, P.R. Coulet. Biosensor Principles and Appli-cations. (Eds.), 357, Marcel Dekker, New York (1991).

[16] D. Ivnitski, A.H. Ihab, A. Plamen, W. Ebtisam, Biosensors for Detection of Pathogenic Bacteria, Biosens. Bioelectron, 14 (1999) 599- 624.

[17] P.T. Kissinger, Biosensors-a Perspective, Biosensors and Bioelectronics, 20 (2005) 2512-2516.

[18] D. Brynn Hibbert, J. Justin Gooding, P. Erokhin, Kinetics of Irreversible Adsorption with Diffusion: Application to Biomolecule Immobilization, Langmuir, 18 (2002), 1770-1776.

[19] I. Langmuir, The Adsorption of Gases on Plane surfaces Glass, Mica and platinum, J. Am. Chem. Soc, 40, (1918) 1361-1403.

[20] Comsol Multiphysics 3.3, www.comsol.com.